7310–7325 *Nucleic Acids Research, 2022, Vol. 50, No. 13* *Published online 1 July 2022*
https://doi.org/10.1093/nar/gkac542

Regulation of both transcription and RNA turnover contribute to germline specification

Kun Tan [1,*] **and Miles F. Wilkinson** [1,2,*]

[1]Department of Obstetrics, Gynecology, and Reproductive Sciences, School of Medicine, University of California San Diego, La Jolla, CA 92093, USA and [2]Institute of Genomic Medicine (IGM), University of California San Diego, La Jolla, CA 92093, USA

Received April 06, 2022; Revised May 29, 2022; Editorial Decision June 07, 2022; Accepted June 29, 2022

ABSTRACT

The nuanced mechanisms driving primordial germ cells (PGC) specification remain incompletely understood since genome-wide transcriptional regulation in developing PGCs has previously only been defined indirectly. Here, using SLAMseq analysis, we determined genome-wide transcription rates during the differentiation of embryonic stem cells (ESCs) to form epiblast-like (EpiLC) cells and ultimately PGC-like cells (PGCLCs). This revealed thousands of genes undergoing bursts of transcriptional induction and rapid shut-off not detectable by RNAseq analysis. Our SLAMseq datasets also allowed us to infer RNA turnover rates, which revealed thousands of mRNAs stabilized and destabilized during PGCLC specification. mRNAs tend to be unstable in ESCs and then are progressively stabilized as they differentiate. For some classes of genes, mRNA turnover regulation collaborates with transcriptional regulation, but these processes oppose each other in a surprisingly high frequency of genes. To test whether regulated mRNA turnover has a physiological role in PGC development, we examined three genes that we found were regulated by RNA turnover: *Sox2, Klf2* and *Ccne1.* Circumvention of their regulated RNA turnover severely impaired the ESC-to-EpiLC and EpiLC-to-PGCLC transitions. Our study demonstrates the functional importance of regulated RNA stability in germline development and provides a roadmap of transcriptional and post-transcriptional regulation during germline specification.

INTRODUCTION

Primordial germ cells (PGCs), the progenitors of gametes, provide the link between one generation and the next. PGC specification, which begins early in the embryo, involves a highly orchestrated combination of transcriptional and epigenetic mechanisms (1–3). While some molecular mechanisms underlying PGC specification *in vivo* have been defined, progress has been hindered by the small number of cells—approximately 40—in the initially formed PGC population (4). Furthermore, most PGC markers are expressed in other cells (5,6), making it difficult to trace PGCs in the developing embryo. A significant advance in the field was the development by Hayashi *et al.* of a defined culture system to generate PGC-like cells (PGCLC) from mouse embryonic stem cells (ESCs) (7). In this model, which closely mimics the events occurring during *in vivo* PGC fate determination, cytokines are used to induce mouse embryonic stem cells (ESCs) to differentiate into epiblast-like cells (EpiLCs), which then are induced to form PGCLCs. As a testament to their similarity to PGCs, these *in vitro*-derived PGCs progress normally through spermatogenesis, generate sperm and, through fertilization, allow for full-term development (7).

PGCLCs have been widely used to study germline fate specification (8–15). For example, this *in vitro* model has recapitulated *in vivo*-defined transcriptional networks critical for PGC specification, such as those involving BLIMP1, PRDM14 and AP2γ (8). Genome-wide CRISPR screens have been performed using PGCLCs to identify transcriptional factors essential for germline fate determination (10). Many mechanistic studies have been done using this *in vitro* model to define transcriptional regulators and circuits important for the PGC specification process (8–15).

While the studies described above identified several transcription factors and downstream genes involved in germline specification, our understanding of the transcriptional networks critical for this developmental process likely remain incomplete. This follows from the fact that the genes identified as being regulated during the germline specification process have been largely defined by RNAseq analysis (7,11,16–19), a method that does not measure transcription rates, but instead measures steady-state mRNA levels. Because RNA steady-state levels reflect not only the amount of newly synthesized mRNA, but also the pre-existing RNA

*To whom correspondence should be addressed. Tel: +1 858 822 4819; Fax: +1 858 822 4701; Email: mfwilkinson@health.ucsd.edu
Correspondence may also be addressed to Kun Tan. Tel: +1 858 405 6496; Fax: +1 858 822 4701; Email: kutan@health.ucsd.edu

pool, transient bursts in transcription would be expected to be invisible to RNAseq analysis. Likewise, the exact timing of the initiation of sustained transcriptional induction events cannot be determined by RNAseq analysis because the pre-existing RNA pool obscures the initial burst of transcription. By the same reasoning, transient or recently-initiated transcriptional silencing events would be expected to escape detection by RNAseq analysis. Thus, the assumption that RNAseq analysis adequately addresses transcriptional regulatory mechanisms is not valid.

Another assumption by many in the field is that developmental events are regulated mainly, if not exclusively, by transcriptional mechanisms coupled with signaling mechanisms (3,20). The tacit assumption is that changes in mRNA levels during development (as detected by RNAseq or qPCR analyses) is primarily due to changes in transcription rate. However, steady-state mRNA levels are also dictated by the rate of mRNA turnover (21,22) (Figure 1A). Regulated mRNA turnover confers regulatory properties that complement transcriptional regulation, such as providing rapid shut-off of gene expression (23). In addition, regulated RNA turnover has the potential to drive precise temporal and spatial control of RNA abundance, particularly during developmental transitions (24). Indeed, empirical studies have shown that regulated RNA turnover influences the expression dynamics of large numbers of transcripts (24–28), often in a cell type-specific or context-dependent manner (26–28).

Despite the potential importance of regulated RNA turnover, only a few studies have identified transcripts regulated by RNA turnover in PGCs. These studies, all of which were conducted in lower organisms (*Drosophila, Danio* and *Oryzias*), identified 3 mRNAs that are selectively stabilized in PGCs (not somatic cells), and other mRNAs whose stability appeared to be regulated by specific RNA-binding proteins in PGCs (29–33). However, the functional consequences of the regulation of these few mRNAs at the level of RNA stability was not determined. Furthermore, to our knowledge, a genome-wide view of mRNAs regulated by turnover in PGCs—in either invertebrates or vertebrates—has not been reported.

In the studies described herein, we measured transcription rates and RNA decay rates genome-wide during the PGC specification process using a metabolic labeling approach called 'thiol(SH)-linked alkylation for the metabolic sequencing of RNA' (SLAMseq) analysis (34). SLAMseq distinguishes newly synthesized and preexisting transcripts by detecting—through chemical conversion—the incorporation of the modified nucleotide, 4-thiouridine (s^4U), into newly synthesized transcripts. SLAMseq analysis allowed us to identify thousands of transcripts undergoing alterations in transcription rate and/or RNA turnover rate during the process of PGC generation. This approach also identified thousands of transcripts undergoing transcriptional alterations not detectable at the steady-state level (by RNAseq analysis). It also defined different classes of genes, including those in which transcription and RNA turnover collaborate to regulate their expression, those in which these two processes antagonize each other, and those in which RNA turnover is the dominant means of regulation. Finally, we addressed a question that has rarely been addressed in any developmental system - does regulated RNA turnover have a functional impact on development? Our experiments designed to address this question allowed us to obtain evidence that specific mRNAs must undergo regulated stabilization and destabilization to permit efficient PGC specification. Together, our study demonstrates the functional importance of regulated RNA turnover, and provides a rich resource for understanding the roles of both transcription and RNA turnover in germline specification.

MATERIALS AND METHODS

Mouse ESC culture and differentiation

Mouse ESCs (V6.5; Novus Biologicals) were maintained on a 0.1% gelatin (MilliporeSigma)-coated dish, under 2i + LIF conditions: N2B27 medium supplemented with 1 × GlutaMAX (Gibco), 1000 U/ml mouse LIF (MilliporeSigma), 3 μM CHIR99021 (MedChem Express) and 1 μM PD0325901 (Selleckchem). Cells were passaged every 3 days.

Mouse ESCs were induced to differentiate into EpiLCs and PGCLCs, as previously described (7). Briefly, three hundred thousand cells were plated on six-well culture plates coated with 16.7 mg/ml fibronectin (MilliporeSigma) and grown in N2B27 medium supplemented with 1% knockout serum replacement (KSR; Gibco), bFGF (12 ng/ml; Life Technologies), and activin A (20 ng/ml; R&D Systems) for 2 days. The medium was changed every day. The PGCLCs were induced under a floating condition by plating two thousand day 2 EpiLCs in a single well from a 96-well Lipidure-Coat Plate (Amsbio) and grown in serum-free GK15 medium (GMEM [Gibco], KSR [15%; Gibco], nonessential amino acids [Gibco], sodium pyruvate [1 mM; Gibco], 2-mercaptoethanol [0.1 mM; Gibco], L-glutamine [2 mM; Gibco], BMP4 [500 ng/ml; Miltenyi Biotec], SCF [100 ng/ml; Miltenyi Biotec], BMP8b [500 ng/ml; R&D Systems], EGF [50 ng/ml; Pepprotech]) and LIF (MilliporeSigma) for 4 days.

Flow cytometry analysis

PGCLCs were purified by cell sorting using antibodies against ITGB3 (Biolegend) and SSEA1 (eBioscience) conjugated with PE and Alexa Fluor 647, respectively, as previously described (35,36). After dissecting single cells, the cells were resuspended in staining buffer (PBS + 3% FBS) for 20 min on ice, stained with the primary antibodies, washed with staining buffer, resuspended in staining buffer and sorted by FACS. Small debris and doublets were removed by gating for size. For negative controls, we analyzed unstained and secondary antibody only (primary omitted) stained cells. The data were processed using FlowJo software (BD Biosciences). Results were from at least three independent replicates. Statistical significance was determined using the paired Student's *t*-test.

SLAMseq analysis

SLAMseq was performed as previously described (34,37). Before collecting samples, the cells were pulse-treated with

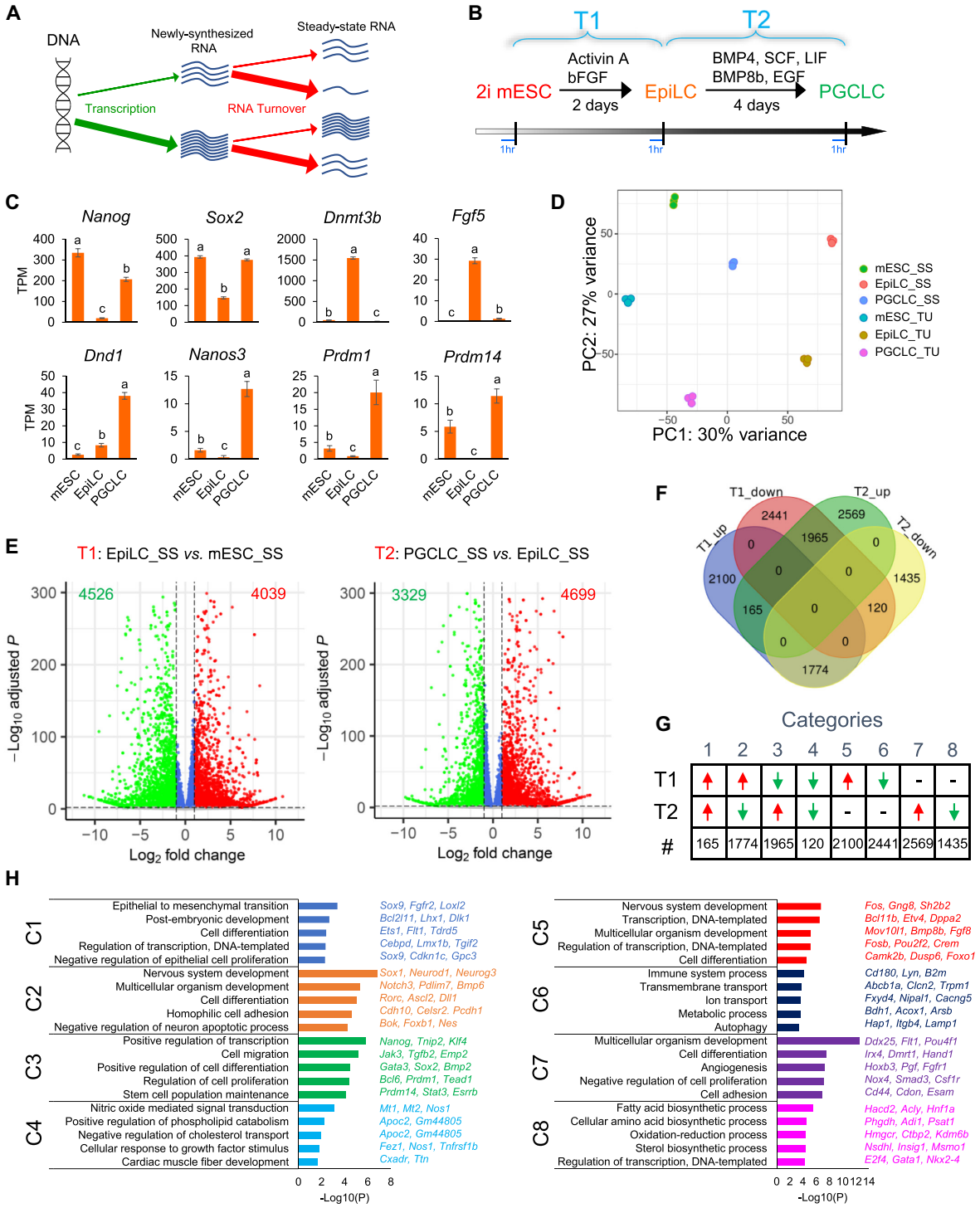

Figure 1. Genome-wide mRNA steady-state level kinetics during the process of PGCLC specification. (**A**) Steady-state mRNA levels are dictated by both RNA synthesis (transcription) and turnover rates. A low transcription rate coupled with high turnover rate yields low mRNA steady-state level (depicted as one transcript), while high transcription rate coupled with low turnover rate yields high mRNA steady-state level (depicted as seven transcripts). An intermediate RNA steady-state level (depicted as three transcripts) can be achieved by either high transcription rate coupled with high RNA turnover rate or the inverse. (**B**) Schematic illustration of the PGCLC specification model. mESC cells cultured under 2i condition are treated with different growth factors, as indicated, to induce their differentiation into EpiLC and PGCLC cells. Before collecting samples for our experiments, cells were given a pulse of s^4U for 1 h. (**C**) The relative expression level ($\log_2$[TPM + 1]) of pluripotency factor genes (*Sox2* and *Nanog*), epiblast marker genes (*Fgf5* and *Dnmt3b*), and PGC-enriched genes (*Prdm1, Prdm14, Nanos3,* and *Dnd1*). Their fold-changes across these three cell stages are shown in Supplementary Table S1. (**D**) PCA of the indicated SLAMseq samples. SS, steady-state RNA; TU, transcription rate. (**E**) Volcano plot showing the steady-state levels of DETs when comparing EpiLCs with mESCs (T1) or PGCLCs with EpiLCs (T2). $q < 0.01$, $|\log_2 FC| > 1$. (**F**) Overlap amongst DETs defined in panel (E). (**G**) The number of transcripts in each of the transcript classes (from panel F). (**H**) The most statistically significant gene ontology (GO) terms for each transcript class (defined in G).

400 μM s^4U for 1 h. After extracting total RNA, carboxyamidomethylation was performed under standard conditions: ∼1–10 μg RNAs, 50% DMSO, 10 mM IAA, 50 mM sodium phosphate buffer (pH 8), incubated for 20 min at 50°C. The reaction was quenched by addition of 1 μl of 1M DTT. After RNA purification, libraries were prepared using the Quant-seq mRNA 3′ end library preparation kit (Lexogen) according to the manufacturer's instructions. Sequencing was performed using a Illumina HiSeq 4000 at the UCSD IGM core in the SR100 mode.

Reads were filtered for quality and aligned with SLAMDUNK (v0.4.3) (38) against the full *Mus musculus* reference genome (GRCm38), with ≤ 100 alignments for multimappers and ≥ 0.2 for sequence variants. Gene and 3′ UTR annotations were obtained from *Ensembl* (https://uswest.ensembl.org/). T > C conversion rate was determined for each position along the custom-defined counting windows by normalizing to genomic T content and coverage of each position and averaging per UTR. Both total read counts (steady-state RNA level) and T > C read counts (transcription; ≥2 T > C conversions) were extracted from SLAMDUNK analysis. Once both steady-state RNA and transcription read counts were normalized to transcripts per kilobase million (TPM), the RNA turnover rate was inferred as previously described (39). Differential gene expression calling was performed using DESeq2 (v1.34.0) (40), using the following threshold: q-value <0.01. The R package program 'pheatmap' was used for clustering and to generate heatmap plots. The database for annotation, visualization and integrated discovery (DAVID) v6.8 was used for GO and pathway analysis.

Transfection and viral transduction

The XRN1-resistant reporter was generated from the pCI-globin_WT-xrRNA vector (Addgene). First, the CMV promoter was replaced with the EF-1α promoter, using the Gibson assembly® kit (NEB). Second, genomic sequences (including the 5′UTR, CDS, intron and 3′UTR regions) from the genes of interest were PCR amplified from genomic DNA and substituted for the β-globin ORF, using the Gibson assembly® kit. Negative control versions of these plasmids lacking the xrRNA-4H sequence were generated using the Q5® site-directed mutagenesis kit (NEB). All insertions and deletions were verified by Sanger sequencing. Plasmids were transiently transfected using the Nucleofector™ kit (Lonza), following the manufacturer's instructions. pEF-globin_WT-xrRNA was co-transfected into cells as an internal control. qPCR detection of RNA turnover was performed as previously described (41). Results were from at least three independent replicates. Statistical significance was determined using the paired Student's t-test.

The *Ccne1-, Klf2-* and *Sox2*-shRNA plasmids were generated by inserting oligonucleotides corresponding to siRNA sequences (Supplementary Table S3) into the pLKO.1 cloning vector (Addgene). The *Ccne1-, Klf2-* and *Sox2* overexpression plasmids were generated by inserting their CDSs into the pFUGW (Addgene) plasmid, using the Gibson assembly® master mix (NEB). For lentiviral transduction, 1 infectious unit (IU) of lentivirus per cell was added with 6 μg/ml polybrene, as described previously (37,42). Results were from at least three independent replicates. Statistical significance was determined using the paired Student's t-test.

qRT-PCR analysis

Total cellular RNA was isolated using TRIzol (Invitrogen), as previously described (43). Quantitative reverse transcription (qRT)-PCR analysis was performed using 1 μg of total cellular RNA using the iScript™ cDNA synthesis kit (Bio-Rad), followed by PCR amplification using SYBR Green (Bio-Rad) (44) and the ΔΔCt method (with ribosomal L19 for normalization). The primers used are listed in Supplementary Table S3. Results were from at least three independent replicates. Statistical significance was determined using the paired Student's t-test.

Immunofluorescence analysis

Immunofluorescence analysis was performed as previously described (7,45,46). The primary antibodies used were as follows: anti-Nanog (eBioscience), anti-DNMT3B (Novus Biologicals), anti-PRDM1 (Novus Biologicals), and anti-NANOS3 (Proteintech). The secondary antibodies used were as follows: Alexa Fluor 488 anti-rat or rabbit IgG, Alexa Fluor 568 anti-rabbit, or -mouse IgG (Thermo Fisher Scientific). The nuclei were counterstained with DAPI (Vector Laboratories), a coverslip was placed over the sections with mounting medium, and the images were viewed using a Leica DMI4000 B fluorescence microscope. Quantification of immunofluorescence signal was performed using NIH ImageJ (1.8.0), as previously described (47).

RESULTS

Steady-state mRNA kinetics during PGCLC specification

To identify genes transcriptionally and post-transcriptionally regulated during the process of PGC specification from pluripotent cells, we used the PGCLC differentiation system described in the Introduction. In this system (7), ESCs are first differentiated into EpiLCs (a developmental transition that we refer to as 'T1') and then these EpiLCs are cultured under conditions to differentiate them into PGCLCs (termed the 'T2' developmental transition) (Figure 1B and Supplementary Figure S1A). We pulse-treated cells from these stages with s^4U and then analyzed the RNA using SLAMseq analysis (Figure 1B and Supplementary Figure S1B), which detects both newly synthesized and steady-state transcripts genome-wide (34). Several parameters were measured to assess SLAMseq data quality: (i) the average number of reads per sample ranged from ∼80 to 94 million, which is more than sufficient to detect transcriptome alterations; (ii) the main conversion of the labelled RNA in response to IAA treatment was thymine-to-cytosine (T > C) (Supplementary Figure S2), as expected given that s^4U is converted to a cytosine analog *via* alkylation (34); (iii) comparison with the negative control (-IAA) demonstrated that s^4U was efficiently incorporated into the samples (∼3–4% *vs* < 0.1% background incorporation; Supplementary Figure S2); (iv) genes encoding pluripotency factors (*Sox2* and *Nanog*),

Epiblast markers (*Fgf5* and *Dnmt3b*), and PGC markers (*Prdm1*, *Prdm14*, *Nanos3* and *Dnd1*), exhibited expression patterns in the 3 stages similar as previously described (Figure 1C, Supplementary Table S1) (7); and (v) principal component analysis (PCA) of triplicate replicates of both steady-state (SS) RNAs and newly synthesized (TU) RNAs exhibited high overlap within groups but clear segregation among different cell types and RNA categories (Figure 1D).

We first used these SLAMseq datasets to define transcripts that undergo statistically-significant shifts in *steady-state level* during the process of PGCLC specification. This analysis identified 8565 differentially expressed transcripts (DETs) between the ESC and EpiLC stages (the T1 transition), and 8028 DETs between the EpiLC and PGCLC stages (the T2 transition) ($q < 0.01$, $|\log_2 FC| > 1$; Figure 1E).

We combined these T1 and T2 datasets to allow us to classify the regulated transcripts into eight categories (Figure 1F, G and Supplementary Table S1). Category 1 (C1) are transcripts upregulated at both the T1 and T2 stages. Among them, *Lhx1, Sox9, Tgif2, Dact1, Fgfr2* and *Tdrd5* have previously been shown to have essential roles in early germ layer specification *in vivo* (48–53). C2 transcripts are enriched at the EpiLC stage as a result of being upregulated and downregulated at the T1 and T2 transitions, respectively. C2 transcripts encode proteins enriched for functions in the Wnt, Notch and MAPK signaling pathways (Supplementary Table S1). C3 transcripts exhibit a biphasic expression pattern, with peak expression in ESCs and PGCLCs, and low expression in EpiLCs. Among the C3 transcripts is *Prdm14,* which encodes a TF essential for the establishment of the germ cell lineage in mice (54). C3 transcripts also encode proteins enriched for functions in the 'signaling pathways regulating pluripotency of stem cells', including the Jak-STAT and Hippo signaling pathways (Supplementary Table S1). C4 transcripts are downregulated at both the T1 and T2 transitions, and thus are highly expressed in ESCs. Among C4 transcripts is *Fst*, which encodes a TGFβ superfamily member that serves as an activin antagonist (55), and thus may repress ESC differentiation into PGCs, as Activin A is known to be crucial for PGCLC formation (56). C5 transcripts are upregulated during the T1 transition and thus are maximally expressed in EpiLCs and/or PGCLCs. C5 transcripts encode proteins enriched for functions in the FoxO, Ras, and estrogen signaling pathways (Supplementary Table S1). C6 transcripts are downregulated during the T1 transition and thus are candidates to be involved in promoting pluripotency. C6 transcripts encode proteins enriched for functions in metabolic pathways and the PI3K-Akt signaling pathway (Supplementary Table S1). C7 transcripts are upregulated during the T2 transition and thus are candidates to specifically be involved in PGCLC specification. C7 transcripts are enriched for proteins involved in the Wnt and TGFβ signaling pathways (Supplementary Table S1), consistent with the evidence that these pathways are required for PGC specification (57,58). Finally, C8 transcripts are downregulated during the T2 transition and thus are candidates to repress PGC specification. C8 transcripts encode proteins involved in the pentose phosphate, glucagon, ErbB, and thyroid hormone signaling pathways (Supplementary Table S1).

Figure 1H shows biological functions statistically enriched in these eight different classes of mRNAs. Some commonalities between classes were observed. For example, C1 and C4 are both enriched in 'epithelial to mesenchymal transition,' 'post-embryonic development,' 'signal transduction,' and 'catabolism' functions. While C1 and C4 are maximally expressed in different stages (PGCLCs and ESCs, respectively), they are both regulated at both the T1 and T2 transitions (Figure 1G), and thus most of the genes in these classes are strongly differentially expressed in ESCs vs. PGCLCs. Since they are oppositely regulated, C1 and C4 are good candidates to encode proteins that oppose each other during PGC differentiation. Similarly, C2 and C3, which are composed of mRNAs regulated in the opposite manner during the T1 and T2 stages (Figure 1G), are both enriched for some of the same functions: 'developmental processes,' 'cell differentiation,' 'transcription,' and 'cell migration.' We conclude that PGC specification *in vitro* is characterized by differentially expression of thousands of mRNAs encoding proteins enriched in specific signaling pathways and functions related to differentiation and development.

Detection of hundreds of transcriptionally-regulated genes, not detectable by RNAseq analysis, during PGCLC specification

While widely used, RNAseq analysis has major limitations for detecting shifts in the rate of transcription. First, RNAseq analysis measures steady-state RNA level, which is dictated not only by transcription rate but also RNA turnover rate. Thus, alterations in gene expression observed by RNAseq can be due to alterations in mRNA stability, not transcription rate. Second, changes in transcription can be obscured by alterations in mRNA stability. For example, if a gene is transcriptionally induced but its encoded mRNA is stabilized, the latter can mask detecting the former. Third, rapid shifts in transcription rate (whether up or down) can be masked by the mass of mRNA present before the transcription rate shift. Thus, it is critical to directly measure transcription rates, which we did using SLAMseq analysis (34).

SLAMseq analysis identified hundreds of genes undergoing significant changes in transcription rate between the ESC and EpiLC stages (4039 and 4119 transcripts are upregulated and downregulated, respectively) (Figure 2A), and between the EpiLC and PGCLC stages (3299 and 2972 transcripts are upregulated and downregulated, respectively) (Figure 2B). Genes undergoing transcriptional upregulation vs. downregulation at each of these two transitions are enriched for different signaling pathways and biological processes (Figure 2A, B). Comparison of this SLAMseq dataset with the conventional RNAseq analysis dataset revealed 3644 transcripts that are differentially transcribed (TU) but whose steady-state (SS) levels are *not* significantly changed between the ESC and EpiLC stages (Figure 2C). Similarly, for the transition between the EpiLC and PGCLC stages, 2965 transcripts are differentially tran-

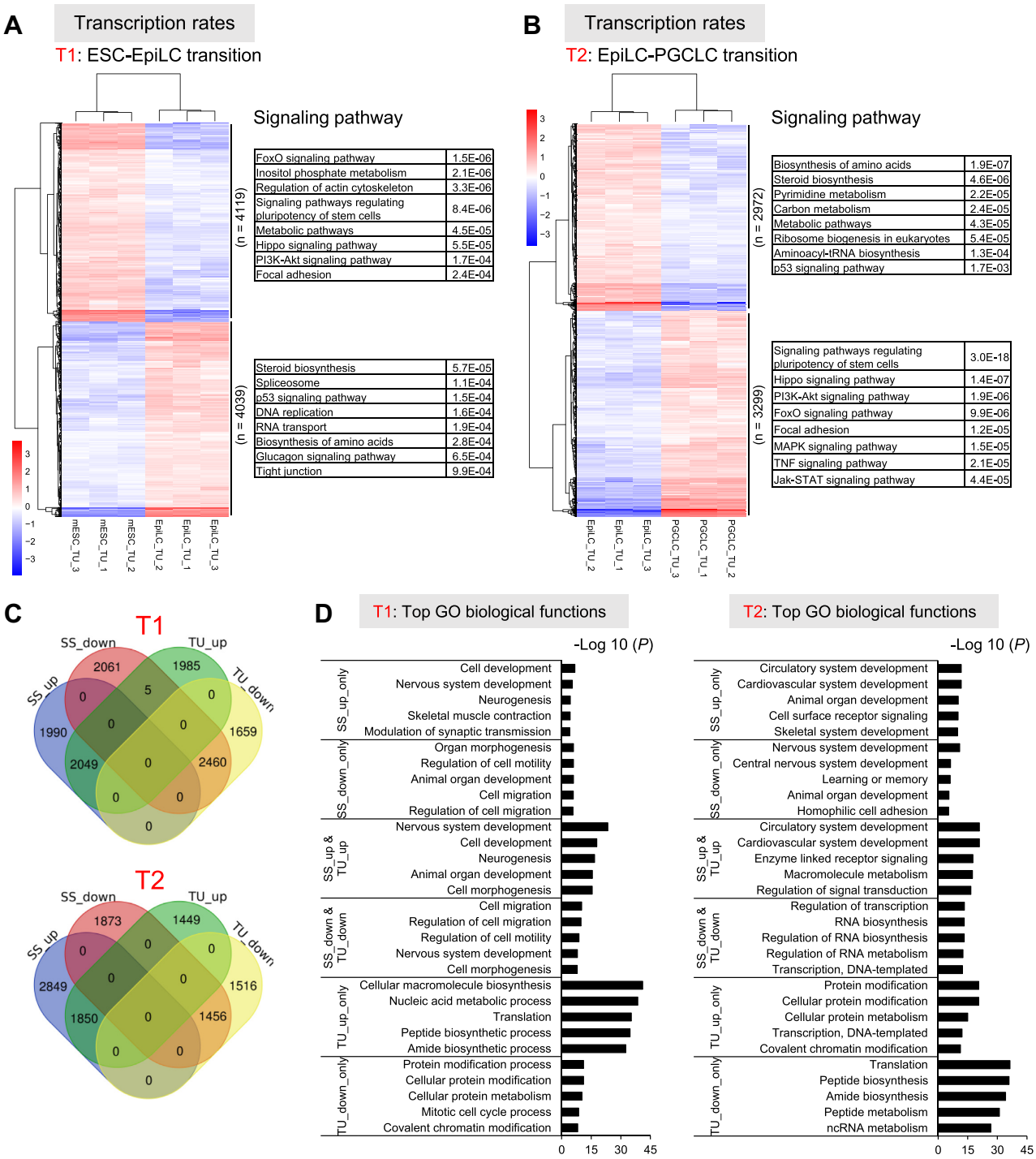

Figure 2. Transcriptionally-regulated genes. (**A**) Left, transcripts undergoing different rates of transcription between mESCs with EpiLCs ($q < 0.01$, $|\log_2 FC| > 0.5$). Three biological replicates from each are shown. Right, most enriched signaling pathways, with P value shown. (**B**) Left, transcripts undergoing different rates of transcription between EpiLCs and PGCLCs, determined as in panel (A). Right, most enriched signaling pathways, with P value shown. (**C**) Overlap of transcripts undergoing changes in steady-state level (SS) and transcription rate (TU). Up, upregulated; down, downregulated. (**D**) Most enriched gene ontology (GO) biological function terms for the transcript classes defined in panel (C).

scribed without a significant change in their steady-state mRNA level (Figure 2C). Thus, this analysis revealed hundreds of genes undergoing transcriptional regulation not detected by RNAseq analysis, thus supported our contention (above) that SLAMseq analysis is a more sensitive measure of transcriptional shifts than RNAseq analysis.

GO analysis showed that transcripts whose regulation is exerted at the steady-state RNA versus the transcriptional level are associated with different biological function terms (Figure 2D). Transcripts only detectably regulated at the steady-state level tend to encode proteins involved in cellular and system developmental processes. In contrast, transcripts only detectably regulated by changes in transcription rate encode proteins involved in metabolic processes, protein modifications, and translation. This indicates that analysis of transcription rates is critical for uncovering the full spectrum of biological functions impacted by development.

The impact of regulated RNA turnover on gene expression during PGC specification

If transcriptional regulation is the major force driving shifts in gene expression during PGC specification, this predicts that most mRNAs undergoing a shift in steady-state level would exhibit a parallel shift in transcription rate. Inconsistent with this model, only ∼half of DETs exhibit a shift in transcription rate (Figure 2C). For example, of the 4039 transcripts upregulated at the steady-state level at T1 (SS_up) only 2049 are transcriptionally upregulated (TU_up) (∼50%). Of the 4699 transcripts upregulated at T2, only 1850 are transcriptionally upregulated (∼39%). Similar values were observed for transcripts downregulated at T1 and T2 (Figure 2C).

This raised the possibility that shifts in RNA turnover is another important parameter that alters steady-state mRNA levels during PGC specification. To address this, we used SLAMseq analysis to infer RNA turnover rates, using the approach described previously (39). This revealed that 2390 and 2112 transcripts are stabilized and destabilized, respectively, as ESCs transition to the EpiLC stage; and 1326 and 1155 transcripts are stabilized and destabilized, respectively, as EpiLCs transition to the PGCLC stage. This indicated that regulated RNA turnover is a significant a contributor to regulation of gene expression during PGC specification.

Analysis of the RNA turnover rate of all detectably expressed transcripts revealed that global RNA turnover rate progressively decreases during the ESC-EpiLC-PGCLC differentiation process ($P < 0.0001$; Figure 3A). Thus, transcripts (as a group) tend to be unstable in ESCs and then become progressively stabilized as ESCs transition to form EpiLCs and then PGCLCs.

To gain insight into the respective roles of RNA turnover and transcription in regulating gene expression during PGCLC specification, we segregated all expressed transcripts into six different classes (Figure 3B, C). Analysis of these classes revealed three distinct roles for RNA turnover during PGC specification. One role of RNA turnover is to drive gene expression. For example, transcripts that are upregulated (at the steady-state level) but do not exhibit a significant change in transcription ('up/-' transcripts) were found to be stabilized as a group during both the T1 and T2 transitions (upward arrow in Figure 3B, C, respectively). Conversely, downregulated transcripts with no change in transcription ('down/-') were found to be destabilized as a group during the T1 transition (downward arrow in Figure 3B).

A second role of RNA turnover is to collaborate with transcription to alter steady-state mRNA levels. In particular, we found that mRNAs transcriptionally upregulated at the T2 transition whose steady-state levels are increased ('up/up') are also stabilized as a group (Figure 3C).

A third role of RNA turnover is to antagonize transcription. Surprisingly, this appeared to be a common role for RNA turnover. For example, all four classes of transcripts with altered transcription rate during the T1 transition ('up/up,' 'down/down,' '-/up,' and '-/down') exhibited an opposite pattern of RNA stabilization (Figure 3B). This raises the possibility that RNA turnover mechanisms are widely employed to dampen the effects of transcriptional changes. Interestingly, RNA turnover and transcription are also opposed for transcripts that are not statistically altered in steady-state level; e.g. the '-/down' class from both the T1 and T2 transitions displayed this regulation (Figure 3B, C, respectively). This suggests that maintenance (no change) of gene expression during development is not always achieved by invariant transcription and RNA turnover rates. Instead, steady-state mRNA levels are often kept constant by shifting transcription and RNA turnover rates in an antagonistic manner that results in no net change in mRNA level. In the Discussion, we speculate on the selection pressures acting over evolutionary time that may be responsible for this 'driving simultaneously with the gas and brakes' pattern of expression.

Considering that RNA-binding proteins (RBPs) exert important roles in regulating RNA stability (59), we determined which RBPs exhibit regulated expression during the T1 and T2 transitions. Of 2889 known RBP genes (60), we found that 256 and 230 are significantly up- and down-regulated, respectively, during the ESC-to-EpiLC transition; and 229 and 258 RBP genes are significantly up- and down-regulated, respectively, during the EpiLC-to-PGCLC transition ($q < 0.01, |\log_2 FC| > 1$; Supplementary Table S2). These differentially regulated RBPs are candidates to be responsible for the shifts in RNA stability of specific transcripts during the process of PGCLC specification.

Transcripts regulated by transcription, RNA turnover, or both

We next segregated *individual* transcripts into different group, depending on their pattern of expression (Figure 4). The group with most members is transcripts undergoing changes in steady-state level that are undergoing a statistically significant change in transcription rate, but not RNA turnover rate. We identified a total of 5281 transcripts in this class (1608, 1962, 1518 and 1268 transcripts upregulated in T1, downregulated in T1, upregulated in T2, and downregulated in T2, respectively; Figure 4A, C, E and G). The large number of transcripts in this class verifies the dogma that transcription plays a major role in regulating gene expression in biological processes (see Discussion).

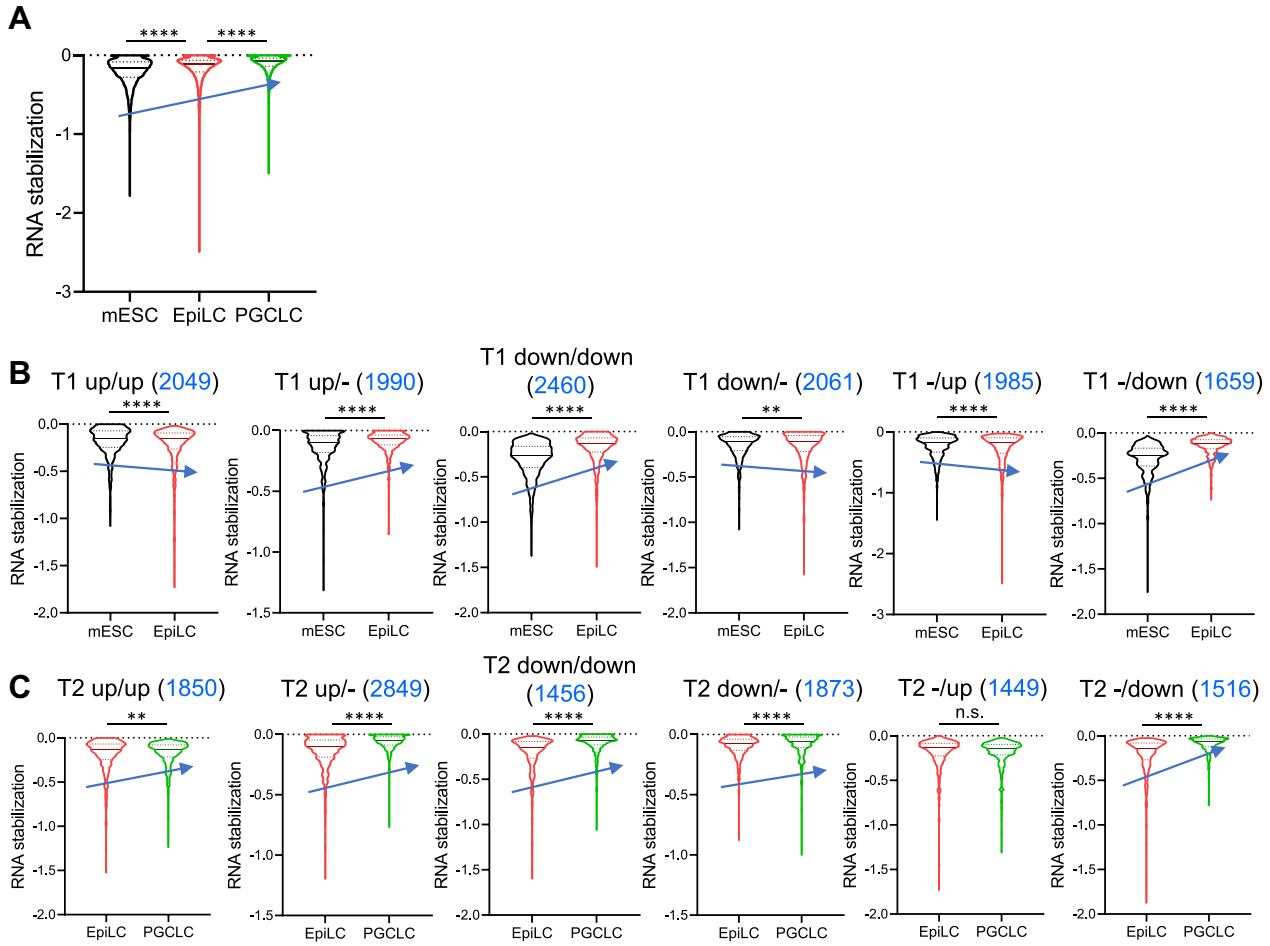

Figure 3. The relationship of RNA synthesis and turnover during PGCLC specification. (**A**) Global RNA turnover rate of all transcripts during PGCLC specification, as inferred from SLAMseq analysis (Supplementary Table S2). The average degree of RNA stabilization is indicated with a solid line; upper quartile and lower quartile RNA turnover rates are indicated with dotted lines. The blue arrow indicates the overall shift in RNA turnover rate, with the upward arrow indicative of a decrease in global RNA turnover as ESCs progress to form EpiLCs and then PGCLCs. (**B**) Shift in RNA turnover rates of the indicated classes of transcripts during the T1 transition, depicted as described in panel A. The first and second terms are the shift in steady-state mRNA level and transcription rate, respectively. Up, upregulated; Down, downregulated; –, no significant change. (**C**) Shift in RNA turnover rates of the indicated classes of transcripts during the T2 transition, depicted as described in panels (A) and (B). $^{**}P < 0.01$; $^{****}P < 0.0001$.

Nonetheless, we also identified 348 transcripts with statistically significant regulation by RNA turnover and not transcription (115, 112, 56 and 80 transcripts whose steady-state levels are upregulated in T1, downregulated in T1, upregulated in T2, and downregulated in T2, respectively; Figure 4A, C, E and G). The role of RNA turnover also extends to transcripts regulated by *both* RNA turnover and transcription. We identified a total of 187 transcripts in this class (43, 87, 45 and 31 transcripts whose steady-state levels are upregulated in T1, downregulated in T1, upregulated in T2, and downregulated in T2, respectively; Figure 4A, C, E, and G). We also found a surprisingly large number of transcripts—1128—are regulated by transcription and RNA turnover in an opposing manner. For example, 398 and 287 transcripts upregulated in T1 and T2, respectively, exhibit increased transcription associated with RNA destabilization (Figure 4A, E); 411 and 157 transcripts downregulated in T1 and T2, respectively, exhibit decreased transcription associated with RNA stabilization (Figure 4C, G). In total, 6273 transcripts undergo a shift in transcription rate and 1639 transcripts undergo a shift in RNA turnover rate during the T1 and T2 transitions.

Figure 4 displays these regulated transcripts segregated into 4 groups, based on their being up- versus downregulated at the steady-state level at the T1 or T2 transition. This reveals different strategies employed by different sets of genes to achieve up- and downregulation. Below we highlight specific genes and gene categories that use these different regulatory strategies during the process of PGC specification:

- *mRNAs upregulated during the ESC-to-EpiLC transition (Figure 1E).* mRNAs upregulated as a result of increased transcription but not a change in RNA turnover rate (Figure 4A) include well-established post-implantation epiblast markers, such as *Dnmt3b, Fgf5, Otx2, Pou3f1 (Oct6)* and *Zic2* (61,62) (Figure 4B). mRNAs instead upregulated as a result of stabilization, not increased transcription (Figure 4A), include *Kdm4c (Jmjd2c)* and *Tcf7l1* (Figure 4B), which have roles in ESC self-renewal

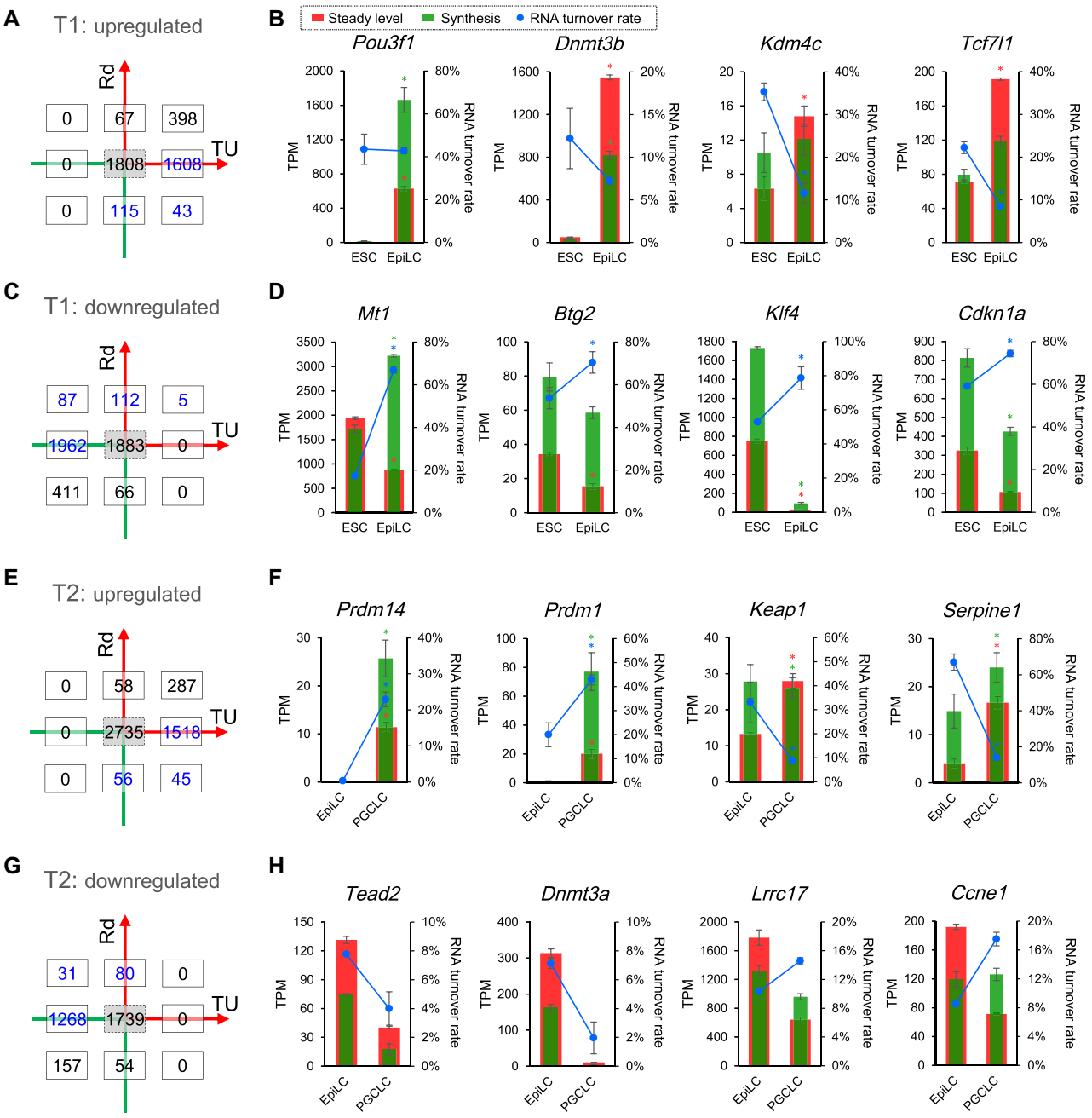

Figure 4. Transcripts stratified by whether they are up- or down-regulated at the steady-state level at the T1 and T2 transitions. (**A**, **C**, **E** and **G**) The number of up and down-regulated transcripts exhibiting changes in transcription (TU) and RNA turnover (Rd) during the T1 and T2 transitions. Numbers in blue refer to transcripts regulated by RNA turnover and/or transcription whose steady-state levels change in the same direction. (**B**, **D**, **F** and **H**) Representative transcripts showing their changes in synthesis, turnover rate, and steady-state level at the stages indicated.

(63) and pluripotent cell lineage specification (64), respectively. mRNAs that are both stabilized and transcriptionally upregulated are involved in several processes, including cell-cell adhesion (*Larp1, Cgn* and *Prdx6*) and the Wnt pathway (*Ccne1, Nxn* and *Tcf7l1*). Upregulated mRNAs oppositely regulated by transcription and RNA turnover (Figure 4A) encode proteins involved with system development, cell differentiation, signal transduction, and cell communication (Supplementary Table S2).

- *mRNAs downregulated during the ESC-to-EpiLC transition (Figure 1E).* Transcriptionally downregulated mRNAs with no change in RNA turnover rate (Figure 4C) are involved in processes such as cell migration, cell motility, cell morphogenesis, and intracellular signal transduction. mRNAs downregulated by destabilization, but not decreased transcription, are involved in metal metabolism and detoxification (*Mt1* and *Mt2*) (Figure 4D), as well as transcriptional regulation, RNA metabolism, and signal transduction. mRNAs both tran-

scriptionally downregulated and destabilized are associated with stemness (*Klf10, Klf4, Sox2, Hes1* and *Hmga2*), cell-cycle arrest (*Cdkn1a, Cdkn1b* and *Kmt2e*), and cell proliferation (*Klf5, Tbx3* and *Pdgfα*) (Figure 4D, Supplementary Table S2). Some downregulated mRNAs are oppositely regulated by transcription and RNA turnover, including *Prdm14* (Supplementary Table S2), an essential factor for PGC specification (54).

- *mRNAs upregulated during the EpiLC-to-PGCLC transition (Figure 1E)*. Transcriptionally upregulated mRNAs not altered in stability (Figure 4E) are involved in signaling pathways regulating pluripotency, germ cell development, cell differentiation, and cell migration. mRNAs upregulated by RNA turnover, not transcription (Figure 4E) are involved in embryonic development (*Tead4, Dlk1, Dlx2, Keap1* and *Kif3a*), signal transduction (*Bambi, Anks1* and *Plaur*), and cell differentiation (*Casz1, Cfl2* and *Tnfrsf12a*) (Figure 4F, Supplementary Table S2). mRNAs both stabilized and transcriptionally upregulated are involved in regulation of apoptosis (*Cdkn1b, Cyr61, Hmgn5, Lefty2* and *Mtch1*) and embryonic development (*Sox2, Tbx3, Fgfr2, Krt8* and *Tgfb2*) (Supplementary Table S2). mRNAs upregulated through increased transcription rate despite being destabilized (Figure 4E) encode proteins involved with signal transduction, tissue morphogenesis, and epithelium development.
- *mRNAs downregulated during the EpiLC-to-PGCLC transition (Figure 1E)*. Transcriptionally downregulated mRNAs undergoing no change in RNA turnover rate (Figure 4G) are involved in transcriptional regulation, DNA methylation, metabolic process, and stem cell differentiation. mRNAs downregulated through destabilization, not decreased transcription (Figure 4G) are involved in cell differentiation (*Ccne1, E2f4, Ifrd1, Lrrc17, Ovol2* and *Tfe3*) and cell development (*Cdh1, Cfl1, Enpp2* and *Zmynd8*) (Figure 4H, Supplementary Table S2). mRNAs that are both transcriptional downregulated and destabilized are associated with intracellular signal transduction (*Atf4, Lmnb1, Pim2* and *Tdgf1*) and RNA metabolic process (*Bend3, Ddx21, Dpy30* and *Top1*) (Supplementary Table S2). mRNAs downregulated through decreased transcription rate despite being stabilized (Figure 4G) encode proteins involved with transcriptional regulation, multicellular organism development, cell differentiation, and covalent chromatin modifications.

Regulated RNA turnover is critical for PGCLC specification

The finding that RNA turnover regulation is responsible for altered steady-state levels of hundreds of transcripts during PGC specification (some of the blue values labelled in Figure 4A, C, E and G) raised the possibility that regulation of RNA turnover is physiologically important for this developmental event. To address this, we elected to focus on the 39 transcripts whose stability is changed at both the T1 and T2 transitions (Figure 5A). Of these 39 transcripts, 22 are stabilized at the T1 stage and then destabilized at the T2 stage; and 17 are destabilized at the T1 stage and then stabilized at the T2 stage. These 39 transcripts are expressed from 22 genes and encode proteins involved in reproductive system development (*Sox2, Tbx3* and *Krt8*), regulation of cell cycle (*Ccne1, Cdkn1b* and *Tex14*), and cell differentiation (*Klf2, Lefty2, Slc25a4* and *Zmynd8*). We selected three of these genes—*Ccne1, Klf2* and *Sox2*—for functional analysis because they have been implicated in regulatory networks in pluripotent cells, which have many characteristics in common with germ cells (65). *Sox2* maintains ESCs in a pluripotent state through regulation of *Oct3/4* expression (66); *Ccne1* exerts key roles in balancing pluripotency and differentiation of ESCs, as well as hematopoietic stem cells (67,68); while *Klf2* functions to accelerate and enhance reversion of mouse epiblast stem cells back to a naive pluripotent state (69). With regard to PGCs, *Sox2* has been shown to be essential for the establishment and maintenance of PGCs *in vivo* (70). While the roles of *Klf2* and *Ccne1* in PGC specification are not known, *Klf2* has been shown to be expressed during PGC specification *in vivo* (71), making it a candidate to have role in this process.

Figure 5B shows the expression pattern of the transcripts from these three genes in ESCs, EpiLCs and PGCLCs. SLAMseq analysis indicated that *Ccne1* mRNA is transiently destabilized during the T1 transition and then stabilized during the T2 transition. Conversely, *Klf2* and *Sox2* mRNA are stabilized during the T1 transition and destabilized in the T2 transition. To validate these expression patterns, we adopted the reporter developed by Voigt *et al.* (41), which contains XRN1-resistant RNA sequences (xrRNAs) in the 3′UTR region of the vector to protect the encoded mRNA from 5′–3′ exonucleolytic digestion (72) (Figure 5C). We cloned genomic sequences from *Ccne1, Klf2,* and *Sox2* (including 5′UTR, CDS, intron, and 3′UTR regions) just upstream of the xrRNA sequence in this vector (Figure 5D). We transiently transfected these constructs into mESCs and assayed the expression of the turnover intermediates at different time points after differentiation. Turnover intermediates were specifically detected by ligating a RNA linker to the free monophosphate on the 5′ end of the turnover intermediates (Figure 5C). qPCR analysis showed that *Ccne1, Klf2* and *Sox2* had the highest levels of RNA turnover intermediates at precisely the same stages that SLAMseq analysis demonstrated that these transcripts were least stable (Figure 5E). As an internal control, we co-transfected a construct expressing β-globin mRNA (Figure 5E). We conclude that *Ccne1, Klf2,* and *Sox2* all exhibit regulated RNA turnover during both the ESC-EpiLC and EpiLC-PGCLC transitions.

The functional importance of regulated RNA turnover of specific mRNAs during development has rarely been previously tested. We examined whether the regulated turnover of the 3 transcripts we selected above is functionally important for PGC specification. To accomplish this, we disrupted their RNA turnover regulation by knocking them down or force expressing them at the stage when they normally undergo regulated RNA turnover.

In the case of *Ccne1* mRNA, we tested the importance of its stabilization during the ESC-to-EpiLC transition (Figure 5B) by knocking it down in ESCs. This knockdown largely extinguished the downregulation of pluripotency genes (*Klf4* and *Nanog*), and it reduced the upregulation of the epiblast-marker genes (*Fgf5* and *Dnmt3b*) (Figure 6A, B). Together, this suggests that the differentiation of ESCs

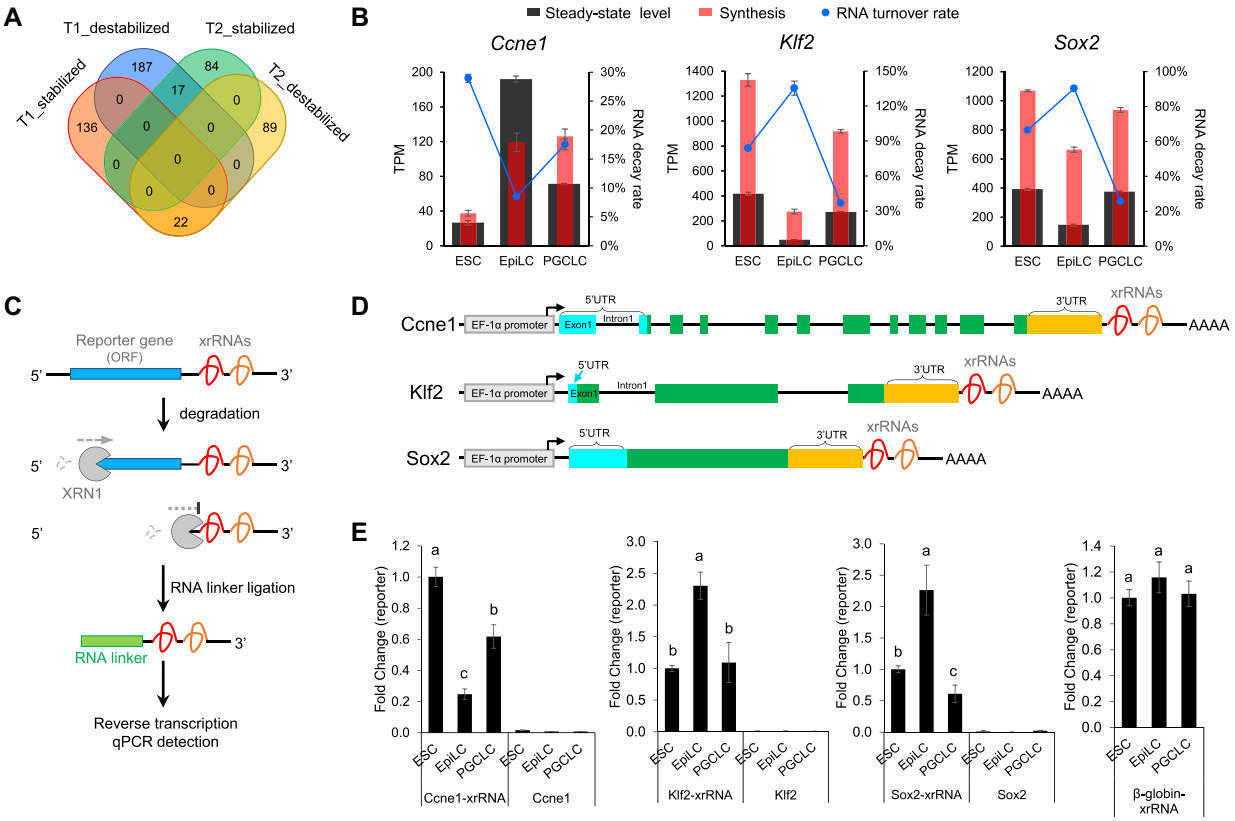

Figure 5. *Cdne1, Klf2*, and *Sox2* transcripts undergo regulated RNA turnover during PGCLC specification. (**A**) Transcripts stabilized and destabilized during both the mESC-EpiLC (T1) and EpiLC-PGCLC (T2) transitions. (**B**) Transcription rate, RNA turnover rate, and steady-state level, as determined by SLAMseq analysis. (**C**) Alternative scheme to determine RNA turnover rates using a plasmid encoding xrRNA sequences that resist 5′ to 3′ exonuclease turnover (e.g. via XRN1). RNA turnover intermediates (generated as a result of 5′ to 3′ exonuclease turnover) harbor a free monophosphate at the 5′ end, which is ligated with an RNA linker to permit detection by qPCR. (**D**) Constructs were generated comprised of genomic sequences from the indicated genes inserted into a vector containing the EF1α promoter and xrRNA sequences downstream. Of note, the polyadenylation site of these three genes was not included in the 3′UTR cloned, forcing usage of the polyadenylation site in the vector (indicted as 'AAAA'). (**E**) qPCR analysis of RNA turnover intermediates in cells at the indicated stages transiently transfected with the indicated constructs depicted in panel D. Constructs lacking the xrRNA sequence were transfected as a negative control. A co-transfected β-globin construct (whose expression was detected by a primer pair specific for β-globin) served as an internal control. Different letters (a, b, c) denote statistically significant differences between different groups ($P < 0.05$).

into EpiLCs is greatly perturbed when the stabilization of *Ccne1* mRNA during the ESC-to-EpiLC transition is prevented.

Conversely, *Ccne1* mRNA is destabilized when EpiLCs are differentiated to form PGCLCs (Figure 5B). To functionally test the importance of this destabilization event, we force expressed *Ccne1* in EpiLCs and found that this reduced the expression of PGCLC-marker genes (Figure 6C, D and Supplementary Figure S3), indicative of lower PGCLC generation efficiency, which we verified by FACS analysis (Figure 6E). Together, these results indicate that (i) the transient expression of *Ccne1* mRNA in EpiLCs is conferred by stage-specific shifts in its turnover rate and (ii) *Ccne1* RNA turnover regulation is critical for efficient PGC specification.

In contrast with *Ccne1*, both *Klf2* and *Sox2* have a bimodal expression pattern, with high expression in ESCs and PGCLCs, but not EpiLCs (Figure 5B). To determine whether the destabilization of these mRNAs during the ESC-to-EpiLC transition is functionally important, we force expressed *Klf2* and *Sox2* in ESCs incubated under conditions that normally generates EpiLCs. This largely prevented the downregulation of pluripotency genes (*Klf4* and *Nanog*), and curtailed the upregulation of epiblast marker genes (*Fgf5* and *Dnmt3b*) (Figure 6A, B). This data indicated that the downregulation of both *Klf2* and *Sox2* mRNA are critical for efficient formation of EpiLCs from ESCs.

To determine whether the stabilization of these mRNAs during the EpiLC-to-PGCLC transition (Figure 5B) is functionally important, we knocked down *Sox2* and *Klf2* in EpiLCs incubated under conditions that normally generates PGCLCs. *Sox2* knockdown significantly reduced the upregulation of PGCLC marker genes (Figure 6C, D), suggesting that *Sox2* mRNA must be upregulated for efficient PGCLC generation. This was confirmed by FACS analysis (Figure 6E). In contrast, *Klf2* knockdown elicited only a modest (non-statistically significant) decrease in PGCLC marker upregulation, as compared to control (Ctrl) group (Figure 6C, D). Accordingly, FACS analysis showed that PGCLC generation frequency was only modestly reduced (Figure 6E). One possible explanation for this modest effect is functional redundancy with other KLF factors, as has been shown for KLF4 and KLF5 (73).

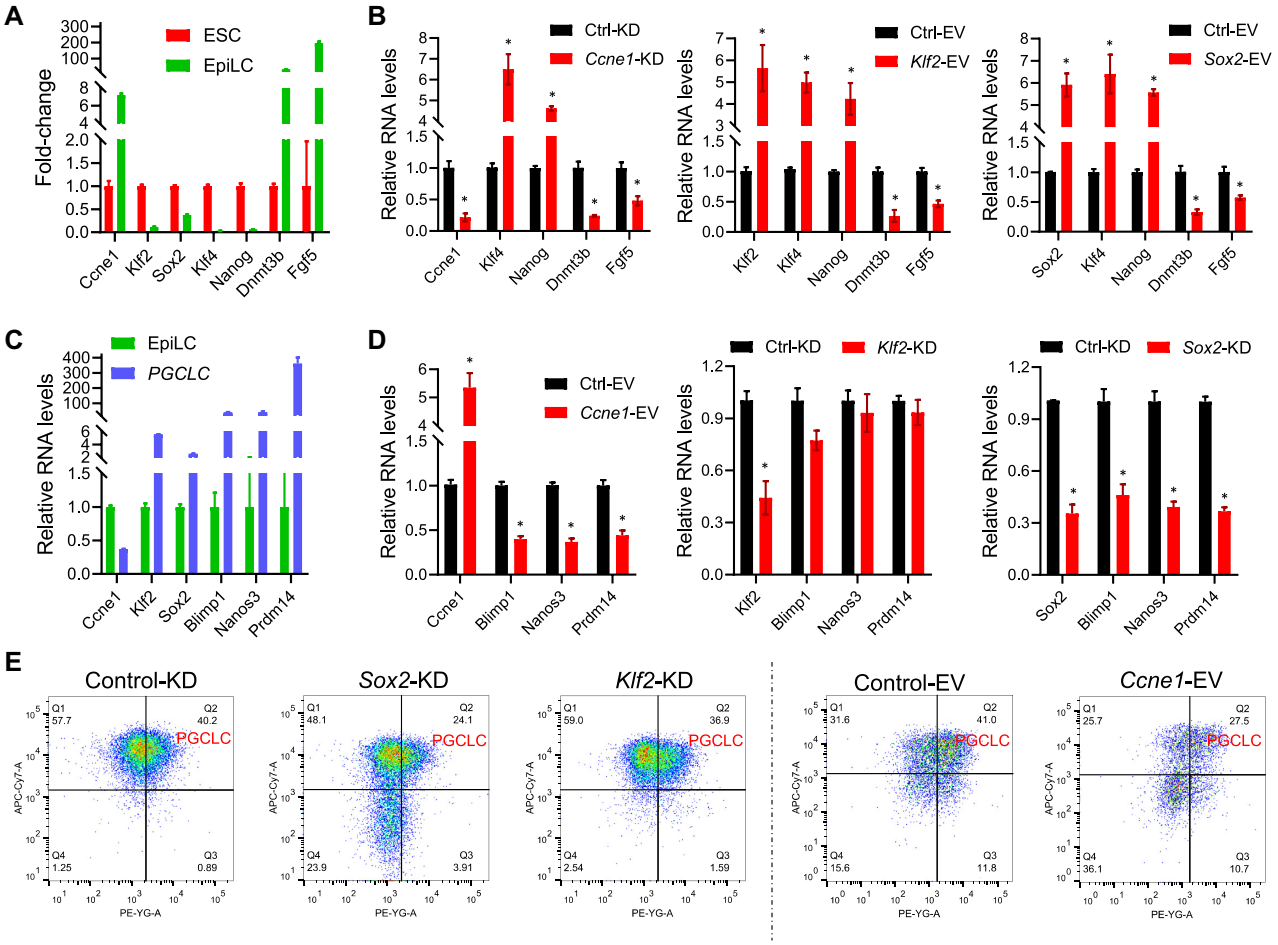

Figure 6. Regulated RNA turnover is critical for PGCLC specification. (**A**) The expression of the indicated genes (steady-state mRNA levels) during the ESC-to-EpiLC transition, as determined by SLAMseq analysis. All values were normalized to expression in ESCs, which was given a value of '1.' (**B**) qPCR analysis of EpiLCs induced from ESCs that were transduced at the ESC stage with the indicated shRNA vectors or expression vectors, respectively. *Ccne1*-KD, *Ccne1* shRNA; Ctrl-KD, negative control (scrambled) shRNA; *Klf2*-EV, *Klf2*-expression vector; *Sox2*-EV, *Sox2*-expression vector; Ctrl-EV, empty expression vector. (**C**) The expression of the indicated genes (steady-state mRNA levels) during the EpiLC-to-PGCLC transition, as determined by SLAMseq analysis. All values were normalized to expression in EpiLCs, which was given a value of '1.' (**D**) qPCR analysis of PGCLCs induced from EpiLCs that were transduced at the EpiLC stage with the indicated shRNA vectors or expression vectors. *Ccne1*-EV, *Ccne1*-expression vector; Ctrl-EV, empty expression vector; *Klf2*-KD, *Klf2* shRNA; *Sox2*-KD, *Sox2* shRNA; Ctrl-KD, negative control (scrambled) shRNA. Statistical significance for panels B and D was determined using the Student's *t* test ($n = 3$). *$P < 0.05$. (**E**) FACS analysis of the proportion of PGCLCs generated under the indicated conditions (defined in panel D). The cells were stained with an antibody against mouse ITGB3 conjugated to PE and an antibody against mouse SSEA1 conjugated to APC. Q2 contains the double-positive (ITGB3$^+$ SSEA1$^+$) PGCLCs (7).

Together, these results show that tight control of the stability of *Ccne1, Sox2* and *Klf2* transcripts is critical for developmental transitions required to generate PGCLCs.

DISCUSSION

Studies elucidating mechanisms driving development have typically focused on transcriptional regulation. This has led to a rich literature demonstrating roles for TFs and other transcriptional regulators in specific developmental steps (74,75). While transcriptional regulation is an intuitively obvious way to change gene expression, regulation of RNA turnover is an equally viable way to alter gene expression and thus this mechanism also has the potential to both influence and direct developmental events. Indeed, studies have indicated that RNA turnover pathways have an impact on many biological events, including some developmental steps (22,76,77). However, the breadth and functional significance of RNA turnover regulation remains largely unknown.

To understand the roles of transcription and RNA turnover in different biological scenarios, it is critical to measure their relative rates genome-wide. Of the few studies that have performed such analyses, most found that transcriptional regulation exerts a stronger overall effect than RNA turnover regulation. For example, it was found that ∼40% and ∼10% of the variance in protein expression in NIH-3T3 fibroblasts is explained by changes in transcription rate and RNA decay rate, respectively (78). More genes were found to be transcriptionally regulated than mRNAs undergoing differential RNA turnover in cytokine-activated human foreskin fibroblasts (79), dendritic cells treated with lipopolysaccharide (80,81), and endothelial cells cultured under hypoxic conditions (82). How-

ever, RNA stability regulation has been found to play a dominant role in some biological scenarios. For example, treatment of NIH-3T3 fibroblasts with the cytokine, interferon, was found to trigger changes in steady-state mRNA levels that correlated well with RNA half-life (83). Another study observed that the majority of mRNAs upregulated at the steady-state level in response to lipopolysaccharide are also stabilized (84). This RNA stabilization response, which was observed in bone marrow-derived monocytes, was found to be temporally regulated and inducer specific (84). Together, these studies demonstrate that both transcription and RNA turnover are regulated in a variety of biological scenarios, but the relative importance of these two pathways appears to depend on the biological context.

To our knowledge, no previous study has determined genome-wide RNA synthesis and turnover rates in a developmental system. In the study herein, we examined transcription and RNA turnover rates—genome-wide—during the process of mouse PGC specification *in vitro*. Previous studies on the topic of RNA turnover in PGCs have only been conducted on isolated mRNAs in non-mammalian species. For example, in fruit flies (*Drosophila*), the well-known translational repressor, NANOS, was reported to destabilize an mRNA of unknown function in PGCs (85). In zebrafish (*Danio*), *nanos1, Tdrd7* and *Hub* mRNA were found to be selectively stabilized in PGCs relative to the soma by virtue of the action of DEADEND, a protein selectively expressed in the germline that represses the action of the maternal mRNA silencer, *miR-430* (30–32). *Tdrd7* mRNA has also been shown to be stabilized in zebrafish PGCs through the action of VASA, which was found to promote *Tdrd7* polyadenylation (86). In Japanese rice fish (*Oryzias*), the stability of *Dmrt1* mRNA was inferred (though observed changes in mRNA level) to be regulated by two RNA-binding proteins (RBPs) that bind to the *Dmrt1* 3′UTR (33). Generality was suggested by the finding that the binding sites for these RBPs are conserved in many species, coupled with the fact that *Dmrt1* is among the most conserved TFs expressed in the germline (87).

Using SLAMseq analysis, we determined the full breadth of RNA turnover regulation in developing mouse PGCs. We identified 1639 transcripts that undergo a statistically significant shift in RNA turnover rate during the process of PGCLC specification. The vast majority of these transcripts underwent a shift in RNA turnover rate at only one of the two developmental steps we examined. Thus, our results indicate that RNA turnover regulation is highly stage specific.

Our analysis also revealed that RNA turnover regulation has different roles. One role is to serve as the primary determinant driving the up- or down-regulation of mRNAs during the process of PGC specification. While a relatively small number of mRNAs are in this class, they encode protein with known roles in ESC self-renewal (*Kdm4c* [*Jmjd2c*]), pluripotent cell lineage specification (*Tcf7l1*), signal transduction (*Bambi, Anks1,* and *Plaur*), cell differentiation (*Casz1, Ccne1, Cfl2, E2f4, Ifrd1, Lrrc17, Ovol2, Tfe3* and *Tnfrsf12a*), embryonic development (*Tead4, Dlk1, Dlx2, Keap1* and *Kif3a*), and cell development in general (*Cdh1, Cfl1, Enpp2* and *Zmynd8*). A second role for regulated RNA turnover is to collaborate with transcriptional regulation to elicit the up- or down-regulation of mRNAs. This collaborative effort leads to the potential to drive a more rapid increase or drop in the expression of proteins than conferred by transcriptional regulation alone. We identified a diverse set of mRNAs in this class. A third role for regulated RNA turnover is to oppose transcriptional regulation. Surprisingly, we identified a large number of mRNAs regulated by this mechanism during PGC specification. This was unexpected, as it seems counter-productive for a cell to, for example, destabilize an mRNA that is being transcriptionally induced. One explanation for this 'drive with the gas and brake' regulatory scenario is it serves as a feedback control mechanism to maintain gene expression. Most shifts in transcription may be of no benefit to the process of PGC specification; they may occur merely because the promoters and/or enhancers in such genes have not been sculpted during evolution to avoid such regulation. In such cases, RNA turnover may serve as a feedback mechanism to prevent a deleterious change in steady-state mRNA level. The converse situation is also possible: shifts in RNA turnover may be opposed by transcriptional feedback control. Both scenarios are supported by our data, as we identified a large number of transcripts (1889) not altered in steady-state level that exhibit opposing changes in transcription rate and turnover rate during PGC specification. We also identified 1128 transcripts that *do* change in steady-state level and are regulated in an opposite manner by transcription and RNA turnover. In the vast majority of these cases, the steady-state level change and transcriptional change are in synch, while RNA turnover is regulated in the opposite direction. Interestingly, many of the mRNAs inversely regulated by transcription and RNA turnover encode proteins involved in 'negative regulation of signal transduction' and 'negative regulation of cell communication'. We speculate that some of these proteins are involved in feedback regulation, and are, in turn, feedback regulated themselves. Finally, we suggest that some mRNAs exhibiting conflicting transcriptional and RNA turnover regulation do so to maintain male germline genome fidelity. This possibility follows from the evidence for a proofreading mechanism operating in the male germline that preferentially couples efficient DNA damage repair with high transcription activity (88). This mechanism may lead to a conflict, as the high levels of some proteins encoded by highly transcribed genes would likely be detrimental to the process of PGC specification. Increased RNA turnover would resolve this conflict by reducing the expression of such toxic proteins without interfering with the fidelity-enhancing benefits of a high transcription rate.

If the regulated turnover of a given mRNA is physiologically important for a developmental process, this predicts that perturbation of this regulation would perturb that developmental process. We elected to test this on three RNA turnover-regulated transcripts identified from our SLAMseq analysis. One of these mRNAs—*Ccne1*—is transiently expressed in EpiLCs by virtue of being stabilized during the ESC-to-EpiLC transition, and then destabilized during the EpiLC-to-PGCLC transition. We found that crippling either *Ccne1* mRNA stabilization or destabilization (by *Ccne1* knockdown or overexpression, respectively, at the appropriate stage) was sufficient to impair PGC specification. These results demonstrated, for the first time, that (i) *Ccne1* is important for PGC development (albeit *in vitro*)

and (ii) its regulation by RNA turnover is critical for *Ccne1* to perform its developmental function. The other two mRNAs we tested—*Sox2* and *Klf2*—have the inverse expression pattern of *Ccne1*: they are maximally expressed at the ESC and PGCLC stages by virtue of being destabilized during the ESC-to-EpiLC transition and stabilized during the EpiLC-to-PGCLC transition. We tested the functional significance of these shifts in RNA turnover and obtained evidence that both shifts in *Sox2* mRNA and at least one of the two shifts in *Klf2* mRNA are critical for normal PGC specification. A caveat of our functional analysis is we only manipulated the levels of *Ccne1, Sox2,* and *Klf2* at the ESC or EpiLC stages. In the future, it would be interesting to define in more detail when precisely these genes must be up- or down-regulated for efficient PGC generation.

Our study also provides a resource for understanding the role of transcription in the process of PGC specification. In particular, SLAMseq analysis identified hundreds of mRNAs regulated by transcription that were not detectably altered at the steady-state mRNA level (i.e. detected by RNAseq analysis). One likely class of such transcripts is those derived from genes undergoing transient shifts in transcription (89). In the future, it will be important to test the functional role of these newly identified transcriptionally-regulated genes in PGC development.

The logic behind regulation by transcription versus RNA turnover remains to be resolved. An advantage of transcriptional control is it is an energetically more favorably way to induce gene expression than stabilizing an already transcribed mRNA. However, transcription is known to require much less energy than translation (24), and thus it is possible that there has been little or no selection pressure to prevent transcription when not immediately needed. Indeed, much of the genome is transcribed in higher eukaryotes with little evidence that most of this is functional (90,91). Thus, it is reasonable that RNA stabilization has become a commonly employed alternative strategy to 'turn on' gene expression. Conversely, RNA *destabilization* is likely to be important for 'turning off' gene expression because it allows for rapid elimination of the protein product (when coupled with rapid transcription shut-off and rapid protein turnover). While rapid gene expression shut-off has been shown to be important in some biological systems, such as the immune response (92), its possible roles in developmental events, such as to confer precise temporal coordination, remains largely untested.

Together, this study defined genome-wide rates of RNA synthesis and turnover in developing PGCs. Our analyses revealed different classes of genes whose levels are controlled by transcription and RNA turnover in a temporally regulated manner in distinct patterns during the process of PGC specification. Through functional studies, we demonstrated that RNA turnover regulation is critical for the process of PGC specification.

DATA AVAILABILITY

The SLAMseq data generated in this study has been deposited at NCBI's GEO database under the accession number: GSE189543.

SUPPLEMENTARY DATA

Supplementary Data are available at NAR Online.

ACKNOWLEDGEMENTS

We thank the UCSD Institute for Genomic Medicine for technical support and the San Diego Supercomputer Center for providing data analysis resources.
Author contributions: K.T. conceived the project. K.T. designed and performed all experiments. K.T. and M.F.W. interpreted the data and wrote the manuscript.

FUNDING

National Institutes of Health [R01 GM119128 and R01 HD093846 to M.F.W.]. Funding for open access charge: National Institutes of Health.
Conflict of interest statement. None declared.

REFERENCES

1. Gunesdogan,U., Magnusdottir,E. and Surani,M.A. (2014) Primordial germ cell specification: a context-dependent cellular differentiation event [corrected]. *Philos. Trans. R. Soc. Lond B. Biol. Sci.*, **369**, 20130543.
2. Hackett,J.A., Zylicz,J.J. and Surani,M.A. (2012) Parallel mechanisms of epigenetic reprogramming in the germline. *Trends Genet.*, **28**, 164–174.
3. Hancock,G.V., Wamaitha,S.E., Peretz,L. and Clark,A.T. (2021) Mammalian primordial germ cell specification. *Development*, **148**, dev189217.
4. Ginsburg,M., Snow,M.H. and McLaren,A. (1990) Primordial germ cells in the mouse embryo during gastrulation. *Development*, **110**, 521–528.
5. O'Connor,M.D., Kardel,M.D., Iosfina,I., Youssef,D., Lu,M., Li,M.M., Vercauteren,S., Nagy,A. and Eaves,C.J. (2008) Alkaline phosphatase-positive colony formation is a sensitive, specific, and quantitative indicator of undifferentiated human embryonic stem cells. *Stem Cells*, **26**, 1109–1116.
6. Mise,N., Fuchikami,T., Sugimoto,M., Kobayakawa,S., Ike,F., Ogawa,T., Tada,T., Kanaya,S., Noce,T. and Abe,K. (2008) Differences and similarities in the developmental status of embryo-derived stem cells and primordial germ cells revealed by global expression profiling. *Genes Cells*, **13**, 863–877.
7. Hayashi,K., Ohta,H., Kurimoto,K., Aramaki,S. and Saitou,M. (2011) Reconstitution of the mouse germ cell specification pathway in culture by pluripotent stem cells. *Cell*, **146**, 519–532.
8. Magnusdottir,E., Dietmann,S., Murakami,K., Gunesdogan,U., Tang,F., Bao,S., Diamanti,E., Lao,K., Gottgens,B. and Azim Surani,M. (2013) A tripartite transcription factor network regulates primordial germ cell specification in mice. *Nat. Cell. Biol.*, **15**, 905–915.
9. Respuela,P., Nikolic,M., Tan,M., Frommolt,P., Zhao,Y., Wysocka,J. and Rada-Iglesias,A. (2016) Foxd3 promotes exit from naive pluripotency through enhancer decommissioning and inhibits germline specification. *Cell. Stem. Cell.*, **18**, 118–133.
10. Hackett,J.A., Huang,Y., Gunesdogan,U., Gretarsson,K.A., Kobayashi,T. and Surani,M.A. (2018) Tracing the transitions from pluripotency to germ cell fate with CRISPR screening. *Nat. Commun.*, **9**, 4292.
11. Kurimoto,K., Yabuta,Y., Hayashi,K., Ohta,H., Kiyonari,H., Mitani,T., Moritoki,Y., Kohri,K., Kimura,H., Yamamoto,T. *et al.* (2015) Quantitative dynamics of chromatin remodeling during germ cell specification from mouse embryonic stem cells. *Cell Stem Cell*, **16**, 517–532.
12. Zhang,M., Ji,J., Wang,X., Zhang,X., Zhang,Y., Li,Y., Wang,X., Li,X., Ban,Q. and Ye,S.D. (2021) The transcription factor tfcp2l1 promotes primordial germ cell-like cell specification of pluripotent stem cells. *J. Biol. Chem.*, **297**, 101217.

13. Yin,Y., Cao,S., Fu,H., Fan,X., Xiong,J., Huang,Q., Liu,Y., Xie,K., Meng,T.G., Liu,Y. *et al.* (2020) A noncanonical role of NOD-like receptor NLRP14 in PGCLC differentiation and spermatogenesis. *Proc. Natl. Acad. Sci. U.S.A.*, **117**, 22237–22248.
14. Zhao,H., Nie,J., Zhu,X., Lu,Y., Liang,X., Xu,H., Yang,X., Zhang,Y., Lu,K. and Lu,S. (2018) In vitro differentiation of spermatogonial stem cell with testicular cells from guangxi bama mini-pig. *J. Vet. Sci.*, **19**, 592–599.
15. Di Giovannantonio,L.G., Acampora,D., Omodei,D., Nigro,V., Barba,P., Barbieri,E., Chambers,I. and Simeone,A. (2021) Direct repression of nanog and oct4 by OTX2 modulates the contribution of epiblast-derived cells to germline and somatic lineage. *Development*, **148**, dev199166.
16. Shirane,K., Kurimoto,K., Yabuta,Y., Yamaji,M., Satoh,J., Ito,S., Watanabe,A., Hayashi,K., Saitou,M. and Sasaki,H. (2016) Global landscape and regulatory principles of DNA methylation reprogramming for germ cell specification by mouse pluripotent stem cells. *Dev. Cell.*, **39**, 87–103.
17. Nakaki,F., Hayashi,K., Ohta,H., Kurimoto,K., Yabuta,Y. and Saitou,M. (2013) Induction of mouse germ-cell fate by transcription factors in vitro. *Nature*, **501**, 222–226.
18. Sasaki,K., Yokobayashi,S., Nakamura,T., Okamoto,I., Yabuta,Y., Kurimoto,K., Ohta,H., Moritoki,Y., Iwatani,C., Tsuchiya,H. *et al.* (2015) Robust in vitro induction of human germ cell fate from pluripotent stem cells. *Cell. Stem. Cell.*, **17**, 178–194.
19. Miyoshi,N., Stel,J.M., Shioda,K., Qu,N., Odajima,J., Mitsunaga,S., Zhang,X., Nagano,M., Hochedlinger,K., Isselbacher,K.J. *et al.* (2016) Erasure of DNA methylation, genomic imprints, and epimutations in a primordial germ-cell model derived from mouse pluripotent stem cells. *Proc. Natl. Acad. Sci. U.S.A.*, **113**, 9545–9550.
20. Cooke,C.B. and Moris,N. (2021) Tissue and cell interactions in mammalian PGC development. *Development*, **148**, dev200093.
21. Alonso,C.R. (2005) Nonsense-mediated RNA decay: a molecular system micromanaging individual gene activities and suppressing genomic noise. *Bioessays*, **27**, 463–466.
22. Yamada,T. and Akimitsu,N. (2019) Contributions of regulated transcription and mRNA decay to the dynamics of gene expression. *Wiley Interdiscip. Rev. RNA*, **10**, e1508.
23. Schoenberg,D.R. and Maquat,L.E. (2012) Regulation of cytoplasmic mRNA decay. *Nat. Rev. Genet.*, **13**, 246–259.
24. Alonso,C.R. (2012) A complex 'mRNA degradation code' controls gene expression during animal development. *Trends Genet.*, **28**, 78–88.
25. Cheadle,C., Fan,J., Cho-Chung,Y.S., Werner,T., Ray,J., Do,L., Gorospe,M. and Becker,K.G. (2005) Control of gene expression during t cell activation: alternate regulation of mRNA transcription and mRNA stability. *BMC Genomics*, **6**, 75.
26. Neff,A.T., Lee,J.Y., Wilusz,J., Tian,B. and Wilusz,C.J. (2012) Global analysis reveals multiple pathways for unique regulation of mRNA decay in induced pluripotent stem cells. *Genome Res.*, **22**, 1457–1467.
27. Munchel,S.E., Shultzaberger,R.K., Takizawa,N. and Weis,K. (2011) Dynamic profiling of mRNA turnover reveals gene-specific and system-wide regulation of mRNA decay. *Mol. Biol. Cell.*, **22**, 2787–2795.
28. Hao,S. and Baltimore,D. (2009) The stability of mRNA influences the temporal order of the induction of genes encoding inflammatory molecules. *Nat. Immunol.*, **10**, 281–288.
29. Barckmann,B. and Simonelig,M. (2013) Control of maternal mRNA stability in germ cells and early embryos. *Biochim. Biophys. Acta.*, **1829**, 714–724.
30. Mishima,Y., Giraldez,A.J., Takeda,Y., Fujiwara,T., Sakamoto,H., Schier,A.F. and Inoue,K. (2006) Differential regulation of germline mRNAs in soma and germ cells by zebrafish miR-430. *Curr. Biol.*, **16**, 2135–2142.
31. Kedde,M., Strasser,M.J., Boldajipour,B., Oude Vrielink,J.A., Slanchev,K., le Sage,C., Nagel,R., Voorhoeve,P.M., van Duijse,J., Orom,U.A. *et al.* (2007) RNA-binding protein dnd1 inhibits microRNA access to target mRNA. *Cell*, **131**, 1273–1286.
32. Mickoleit,M., Banisch,T.U. and Raz,E. (2011) Regulation of hub mRNA stability and translation by miR430 and the dead end protein promotes preferential expression in zebrafish primordial germ cells. *Dev. Dyn.*, **240**, 695–703.
33. Herpin,A., Schmidt,C., Kneitz,S., Gobe,C., Regensburger,M., Le Cam,A., Montfort,J., Adolfi,M.C., Lillesaar,C., Wilhelm,D. *et al.* (2019) A novel evolutionary conserved mechanism of RNA stability regulates synexpression of primordial germ cell-specific genes prior to the sex-determination stage in medaka. *PLoS Biol.*, **17**, e3000185.
34. Herzog,V.A., Reichholf,B., Neumann,T., Rescheneder,P., Bhat,P., Burkard,T.R., Wlotzka,W., von Haeseler,A., Zuber,J. and Ameres,S.L. (2017) Thiol-linked alkylation of RNA to assess expression dynamics. *Nat. Methods*, **14**, 1198–1204.
35. Sohni,A., Tan,K., Song,H.-W., Burow,D., de Rooij,D.G., Laurent,L., Hsieh,T.-C., Rabah,R., Hammoud,S.S. and Vicini,E. (2019) The neonatal and adult human testis defined at the single-cell level. *Cell Rep.*, **26**, 1501–1517.
36. Tan,K., Song,H.-W., Thompson,M., Munyoki,S., Sukhwani,M., Hsieh,T.-C., Orwig,K.E. and Wilkinson,M.F. (2020) Transcriptome profiling reveals signaling conditions dictating human spermatogonia fate in vitro. *Proceedings of the National Academy of Sciences*, **117**, 17832–17841.
37. Tan,K., Song,H.W. and Wilkinson,M.F. (2021) RHOX10 drives mouse spermatogonial stem cell establishment through a transcription factor signaling cascade. *Cell Rep.*, **36**, 109423.
38. Neumann,T., Herzog,V.A., Muhar,M., von Haeseler,A., Zuber,J., Ameres,S.L. and Rescheneder,P. (2019) Quantification of experimentally induced nucleotide conversions in high-throughput sequencing datasets. *BMC Bioinformatics*, **20**, 258.
39. Jurges,C., Dolken,L. and Erhard,F. (2018) Dissecting newly transcribed and old RNA using GRAND-SLAM. *Bioinformatics*, **34**, i218–i226.
40. Love,M.I., Huber,W. and Anders,S. (2014) Moderated estimation of fold change and dispersion for RNA-seq data with DESeq2. *Genome Biol.*, **15**, 550.
41. Voigt,F., Gerbracht,J.V., Boehm,V., Horvathova,I., Eglinger,J., Chao,J.A. and Gehring,N.H. (2019) Detection and quantification of RNA decay intermediates using XRN1-resistant reporter transcripts. *Nat. Protoc.*, **14**, 1603–1633.
42. Tan,K., Kim,M.E., Song,H.W., Skarbrevik,D., Babajanian,E., Bedrosian,T.A., Gage,F.H. and Wilkinson,M.F. (2021) The rhox gene cluster suppresses germline LINE1 transposition. *Proc. Natl. Acad. Sci. U.S.A.*, **118**, e2024785118.
43. Ramaiah,M., Tan,K., Plank,T.M., Song,H.W., Dumdie,J.N., Jones,S., Shum,E.Y., Sheridan,S.D., Peterson,K.J., Gromoll,J. *et al.* (2019) A microRNA cluster in the Fragile-X region expressed during spermatogenesis targets FMR1. *EMBO Rep.*, **20**, e46566.
44. Tan,K., An,L., Miao,K., Ren,L., Hou,Z., Tao,L., Zhang,Z., Wang,X., Xia,W. and Liu,J. (2016) Impaired imprinted x chromosome inactivation is responsible for the skewed sex ratio following in vitro fertilization. *Proc. Natl. Acad. Sci. U.S.A.*, **113**, 3197–3202.
45. Tan,K., Song,H.W. and Wilkinson,M.F. (2020) Single-cell RNAseq analysis of testicular germ and somatic cell development during the perinatal period. *Development*, **147**, dev183251.
46. Tan,K., Jones,S.H., Lake,B.B., Dumdie,J.N., Shum,E.Y., Zhang,L., Chen,S., Sohni,A., Pandya,S., Gallo,R.L. *et al.* (2020) The Role of the NMD Factor UPF3B in Olfactory Sensory Neurons. *Elife*, **9**, e57525.
47. Tan,K., An,L., Wang,S.M., Wang,X.D., Zhang,Z.N., Miao,K., Sui,L.L., He,S.Z., Nie,J.Z., Wu,Z.H. *et al.* (2015) Actin disorganization plays a vital role in impaired embryonic development of in vitro-produced mouse preimplantation embryos. *PLoS One*, **10**, e0130382.
48. Costello,I., Nowotschin,S., Sun,X., Mould,A.W., Hadjantonakis,A.K., Bikoff,E.K. and Robertson,E.J. (2015) Lhx1 functions together with otx2, foxa2, and ldb1 to govern anterior mesendoderm, node, and midline development. *Genes Dev.*, **29**, 2108–2122.
49. Yamamizu,K., Schlessinger,D. and Ko,M.S. (2014) SOX9 accelerates ESC differentiation to three germ layer lineages by repressing SOX2 expression through P21 (WAF1/CIP1). *Development*, **141**, 4254–4266.
50. Powers,S.E., Taniguchi,K., Yen,W., Melhuish,T.A., Shen,J., Walsh,C.A., Sutherland,A.E. and Wotton,D. (2010) Tgif1 and tgif2 regulate nodal signaling and are required for gastrulation. *Development*, **137**, 249–259.
51. Suriben,R., Kivimae,S., Fisher,D.A., Moon,R.T. and Cheyette,B.N. (2009) Posterior malformations in dact1 mutant mice arise through misregulated vangl2 at the primitive streak. *Nat. Genet.*, **41**, 977–985.
52. Arman,E., Haffner-Krausz,R., Chen,Y., Heath,J.K. and Lonai,P. (1998) Targeted disruption of fibroblast growth factor (FGF) receptor 2 suggests a role for FGF signaling in pregastrulation mammalian development. *Proc. Natl. Acad. Sci. U.S.A.*, **95**, 5082–5087.

53. Yabuta,Y., Ohta,H., Abe,T., Kurimoto,K., Chuma,S. and Saitou,M. (2011) TDRD5 is required for retrotransposon silencing, chromatoid body assembly, and spermiogenesis in mice. *J. Cell. Biol.*, **192**, 781–795.
54. Yamaji,M., Seki,Y., Kurimoto,K., Yabuta,Y., Yuasa,M., Shigeta,M., Yamanaka,K., Ohinata,Y. and Saitou,M. (2008) Critical function of prdm14 for the establishment of the germ cell lineage in mice. *Nat. Genet.*, **40**, 1016–1022.
55. Sugino,K., Kurosawa,N., Nakamura,T., Takio,K., Shimasaki,S., Ling,N., Titani,K. and Sugino,H. (1993) Molecular heterogeneity of follistatin, an activin-binding protein. Higher affinity of the carboxyl-terminal truncated forms for heparan sulfate proteoglycans on the ovarian granulosa cell. *J. Biol. Chem.*, **268**, 15579–15587.
56. Sun,R., Sun,Y.C., Ge,W., Tan,H., Cheng,S.F., Yin,S., Sun,X.F., Li,L., Dyce,P., Li,J. *et al.* (2015) The crucial role of activin a on the formation of primordial germ cell-like cells from skin-derived stem cells in vitro. *Cell Cycle*, **14**, 3016–3029.
57. Aramaki,S., Hayashi,K., Kurimoto,K., Ohta,H., Yabuta,Y., Iwanari,H., Mochizuki,Y., Hamakubo,T., Kato,Y., Shirahige,K. *et al.* (2013) A mesodermal factor, t, specifies mouse germ cell fate by directly activating germline determinants. *Dev. Cell*, **27**, 516–529.
58. Ohinata,Y., Ohta,H., Shigeta,M., Yamanaka,K., Wakayama,T. and Saitou,M. (2009) A signaling principle for the specification of the germ cell lineage in mice. *Cell*, **137**, 571–584.
59. Hentze,M.W., Castello,A., Schwarzl,T. and Preiss,T. (2018) A brave new world of RNA-binding proteins. *Nat. Rev. Mol. Cell. Biol.*, **19**, 327–341.
60. Caudron-Herger,M., Jansen,R.E., Wassmer,E. and Diederichs,S. (2021) RBP2GO: a comprehensive pan-species database on RNA-binding proteins, their interactions and functions. *Nucleic Acids Res.*, **49**, D425–D436.
61. Subramanian,A., Tamayo,P., Mootha,V.K., Mukherjee,S., Ebert,B.L., Gillette,M.A., Paulovich,A., Pomeroy,S.L., Golub,T.R., Lander,E.S. *et al.* (2005) Gene set enrichment analysis: a knowledge-based approach for interpreting genome-wide expression profiles. *Proc. Natl. Acad. Sci. U.S.A.*, **102**, 15545–15550.
62. Folmes,C.D., Dzeja,P.P., Nelson,T.J. and Terzic,A. (2012) Metabolic plasticity in stem cell homeostasis and differentiation. *Cell Stem Cell*, **11**, 596–606.
63. Pedersen,M.T., Kooistra,S.M., Radzisheuskaya,A., Laugesen,A., Johansen,J.V., Hayward,D.G., Nilsson,J., Agger,K. and Helin,K. (2016) Continual removal of H3K9 promoter methylation by jmjd2 demethylases is vital for ESC self-renewal and early development. *EMBO J.*, **35**, 1550–1564.
64. Hoffman,J.A., Wu,C.I. and Merrill,B.J. (2013) Tcf7l1 prepares epiblast cells in the gastrulating mouse embryo for lineage specification. *Development*, **140**, 1665–1675.
65. Reik,W. and Surani,M.A. (2015) Germline and pluripotent stem cells. *Cold Spring Harb Perspect. Biol.*, **7**, a019422.
66. Masui,S., Nakatake,Y., Toyooka,Y., Shimosato,D., Yagi,R., Takahashi,K., Okochi,H., Okuda,A., Matoba,R., Sharov,A.A. *et al.* (2007) Pluripotency governed by sox2 via regulation of oct3/4 expression in mouse embryonic stem cells. *Nat. Cell. Biol.*, **9**, 625–635.
67. Campaner,S., Viale,A., De Fazio,S., Doni,M., De Franco,F., D'Artista,L., Sardella,D., Pelicci,P.G. and Amati,B. (2013) A non-redundant function of cyclin E1 in hematopoietic stem cells. *Cell Cycle*, **12**, 3663–3672.
68. Krivega,M.V., Geens,M., Heindryckx,B., Santos-Ribeiro,S., Tournaye,H. and Van de Velde,H. (2015) Cyclin E1 plays a key role in balancing between totipotency and differentiation in human embryonic cells. *Mol. Hum. Reprod.*, **21**, 942–956.
69. Gillich,A., Bao,S., Grabole,N., Hayashi,K., Trotter,M.W., Pasque,V., Magnusdottir,E. and Surani,M.A. (2012) Epiblast stem cell-based system reveals reprogramming synergy of germline factors. *Cell Stem Cell*, **10**, 425–439.
70. Campolo,F., Gori,M., Favaro,R., Nicolis,S., Pellegrini,M., Botti,F., Rossi,P., Jannini,E.A. and Dolci,S. (2013) Essential role of sox2 for the establishment and maintenance of the germ cell line. *Stem Cells*, **31**, 1408–1421.
71. Saitou,M. and Yamaji,M. (2012) Primordial germ cells in mice. *Cold Spring Harb. Perspect. Biol.*, **4**, a008375.
72. Chang,C.T., Bercovich,N., Loh,B., Jonas,S. and Izaurralde,E. (2014) The activation of the decapping enzyme DCP2 by DCP1 occurs on the EDC4 scaffold and involves a conserved loop in DCP1. *Nucleic Acids Res.*, **42**, 5217–5233.
73. Jiang,J., Chan,Y.S., Loh,Y.H., Cai,J., Tong,G.Q., Lim,C.A., Robson,P., Zhong,S. and Ng,H.H. (2008) A core klf circuitry regulates self-renewal of embryonic stem cells. *Nat. Cell. Biol.*, **10**, 353–360.
74. Lewis,M. and Stracker,T.H. (2021) Transcriptional regulation of multiciliated cell differentiation. *Semin. Cell. Dev. Biol.*, **110**, 51–60.
75. Grosveld,F., van Staalduinen,J. and Stadhouders,R. (2021) Transcriptional regulation by (Super)Enhancers: from discovery to mechanisms. *Annu. Rev. Genomics Hum. Genet.*, **22**, 127–146.
76. Keene,J.D. (2010) Minireview: global regulation and dynamics of ribonucleic acid. *Endocrinology*, **151**, 1391–1397.
77. Jaffrey,S.R. and Wilkinson,M.F. (2018) Nonsense-mediated RNA decay in the brain: emerging modulator of neural development and disease. *Nat. Rev. Neurosci.*, **19**, 715–728.
78. Schwanhausser,B., Busse,D., Li,N., Dittmar,G., Schuchhardt,J., Wolf,J., Chen,W. and Selbach,M. (2011) Global quantification of mammalian gene expression control. *Nature*, **473**, 337–342.
79. Paulsen,M.T., Veloso,A., Prasad,J., Bedi,K., Ljungman,E.A., Tsan,Y.C., Chang,C.W., Tarrier,B., Washburn,J.G., Lyons,R. *et al.* (2013) Coordinated regulation of synthesis and stability of RNA during the acute TNF-induced proinflammatory response. *Proc. Natl. Acad. Sci. U.S.A.*, **110**, 2240–2245.
80. Rabani,M., Levin,J.Z., Fan,L., Adiconis,X., Raychowdhury,R., Garber,M., Gnirke,A., Nusbaum,C., Hacohen,N., Friedman,N. *et al.* (2011) Metabolic labeling of RNA uncovers principles of RNA production and degradation dynamics in mammalian cells. *Nat. Biotechnol.*, **29**, 436–442.
81. Rabani,M., Raychowdhury,R., Jovanovic,M., Rooney,M., Stumpo,D.J., Pauli,A., Hacohen,N., Schier,A.F., Blackshear,P.J., Friedman,N. *et al.* (2014) High-resolution sequencing and modeling identifies distinct dynamic RNA regulatory strategies. *Cell*, **159**, 1698–1710.
82. Tiana,M., Acosta-Iborra,B., Hernandez,R., Galiana,C., Fernandez-Moreno,M.A., Jimenez,B. and Del Peso,L. (2020) Metabolic labeling of RNA uncovers the contribution of transcription and decay rates on hypoxia-induced changes in RNA levels. *RNA*, **26**, 1006–1022.
83. Dolken,L., Ruzsics,Z., Radle,B., Friedel,C.C., Zimmer,R., Mages,J., Hoffmann,R., Dickinson,P., Forster,T., Ghazal,P. *et al.* (2008) High-resolution gene expression profiling for simultaneous kinetic parameter analysis of RNA synthesis and decay. *RNA*, **14**, 1959–1972.
84. Hao,H.N., Peduzzi-Nelson,J.D., VandeVord,P.J., Barami,K., DeSilva,S.P., Pelinkovic,D. and Morawa,L.G. (2009) Lipopolysaccharide-induced inflammatory cytokine production by schwann's cells dependent upon TLR4 expression. *J. Neuroimmunol.*, **212**, 26–34.
85. Sugimori,S., Kumata,Y. and Kobayashi,S. (2018) Maternal nanos-dependent RNA stabilization in the primordial germ cells of drosophila embryos. *Dev. Growth Differ.*, **60**, 63–75.
86. Takeda,Y., Mishima,Y., Fujiwara,T., Sakamoto,H. and Inoue,K. (2009) DAZL relieves miRNA-mediated repression of germline mRNAs by controlling poly(A) tail length in zebrafish. *PLoS One*, **4**, e7513.
87. Zarkower,D. (2013) DMRT genes in vertebrate gametogenesis. *Curr. Top Dev. Biol.*, **102**, 327–356.
88. Xia,B., Yan,Y., Baron,M., Wagner,F., Barkley,D., Chiodin,M., Kim,S.Y., Keefe,D.L., Alukal,J.P., Boeke,J.D. *et al.* (2020) Widespread transcriptional scanning in the testis modulates gene evolution rates. *Cell*, **180**, 248–262.
89. Swift,J. and Coruzzi,G.M. (2017) A matter of time - How transient transcription factor interactions create dynamic gene regulatory networks. *Biochim. Biophys. Acta. Gene. Regul. Mech.*, **1860**, 75–83.
90. Core,L.J., Waterfall,J.J. and Lis,J.T. (2008) Nascent RNA sequencing reveals widespread pausing and divergent initiation at human promoters. *Science*, **322**, 1845–1848.
91. Kindgren,P., Ivanov,M. and Marquardt,S. (2020) Native elongation transcript sequencing reveals temperature dependent dynamics of nascent RNAPII transcription in arabidopsis. *Nucleic Acids Res.*, **48**, 2332–2347.
92. Khabar,K.S. (2007) Rapid transit in the immune cells: the role of mRNA turnover regulation. *J. Leukoc. Biol.*, **81**, 1335–1344.